

Trace Detection of Tetrahydrocannabinol in Body Fluid via Surface-Enhanced Raman Scattering and Principal Component Analysis

Kundan Sivashanmugan,[†] Kenneth Squire,[†] Ailing Tan,^{†,§} Yong Zhao,^{†,||} Joseph Abraham Kraai,[‡] Gregory L. Rorrer,[‡] and Alan X. Wang^{*,†,ID}

[†]School of Electrical Engineering and Computer Science and [‡]School of Chemical, Biological, and Ecological Engineering, Oregon State University, Corvallis, Oregon 97331, United States

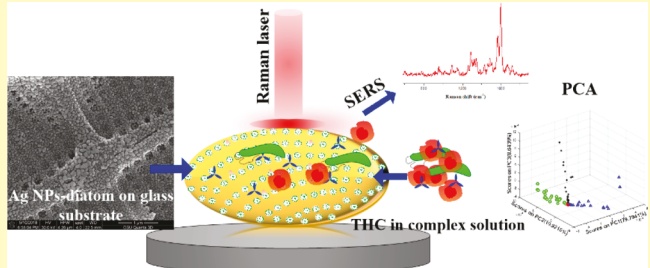
[§]School of Information Science and Engineering, The Key Laboratory for Special Fiber and Fiber Sensor of Hebei Province, and

^{||}School of Electrical Engineering, The Key Laboratory of Measurement Technology and Instrumentation of Hebei Province, Yanshan University, Qinhuangdao 066004, China

Supporting Information

ABSTRACT: Tetrahydrocannabinol (THC) is the main active component in marijuana and the rapid detection of THC in human body fluid plays a critical role in forensic analysis and public health. Surface-enhanced Raman scattering (SERS) sensing has been increasingly used to detect illicit drugs; however, only limited SERS sensing results of THC in methanol solution have been reported, while its presence in body fluids, such as saliva or plasma, has yet to be investigated. In this article, we demonstrate the trace detection of THC in human plasma and saliva solution using a SERS-active substrate formed by *in situ* growth of silver nanoparticles (Ag NPs) on diatom frustules. THC at extremely low concentration of 1 pM in plasma and purified saliva solutions were adequately distinguished with good reproducibility. The SERS peak at 1603 cm^{-1} with standard deviation of 3.4 cm^{-1} was used for the evaluation of THC concentration in a methanol solution. Our SERS measurement also shows that this signature peak experiences a noticeable wavenumber shift and a slightly wider variation in the plasma and saliva solution. Additionally, we observed that THC in plasma or saliva samples produces a strong SERS peak at 1621 cm^{-1} due to the stretching mode of $\text{O}-\text{C}=\text{O}$, which is related to the metabolic change of THC structures in body fluid. To conduct a quantitative analysis, principal component analysis (PCA) was applied to analyze the SERS spectra of 1 pM THC in methanol solution, plasma, and purified saliva samples. The maximum variability of the first three principal components was achieved at 71%, which clearly denotes the impact of different biological background signals. Similarly, the SERS spectra of THC in raw saliva solution under various metabolic times were studied using PCA and 98% of the variability is accounted for in the first three principal components. The clear separation of samples measured at different THC resident times can provide time-dependent information on the THC metabolic process in body fluids. A linear regression model was used to estimate the metabolic rate of THC in raw saliva and the predicted metabolic time in the testing data set matched well with the training data set. In summary, the hybrid plasmonic-biosilica SERS substrate can achieve ultrasensitive, near-quantitative detection of trace levels of THC in complex body fluids, which can potentially transform forensic sensing techniques to detect marijuana abuse.

KEYWORDS: tetrahydrocannabinol, surface-enhanced Raman scattering, plasmonic nanoparticles, diatoms, drug abuse



The abuse of psychoactive drugs has caused serious health problems and a rise in criminal activity in recent years.^{1–4} Cannabis, also known as marijuana, is one of the most commonly used psychoactive drugs for medical or recreational purposes.^{5–7} The most common short-term physical and neurological effects of cannabis include increased heart rate, increased appetite, reduced blood pressure, impairment of short-term and working memory, psychomotor coordination, and concentration.^{3,5,8–14} Cannabis contains more than 60 psychoactive cannabinoids^{3,5,8,9} including the most controversial component, Δ^9 -tetrahydrocannabinol (THC), which is responsible for hallucinogenic effects.^{3,5,8–13,15,16} In human body fluid, THC is rapidly oxidized into a hydroxyl metabolite

(OH-THC) and a carboxylic acid metabolite (THC-COOH), which are nonpsychoactive but can be present in blood and urine for multiple days after the use of cannabis.^{3,5,8–13,16} Therefore, trace detection of THC and its metabolic products in body fluid is critical to prevent drug abuse and improve forensic investigation of driving under the influence (DUI) or other criminal offenses.

Received: March 8, 2019

Accepted: March 25, 2019

Published: March 25, 2019



(a) Electroless deposition of Ag NPs on diatom surface

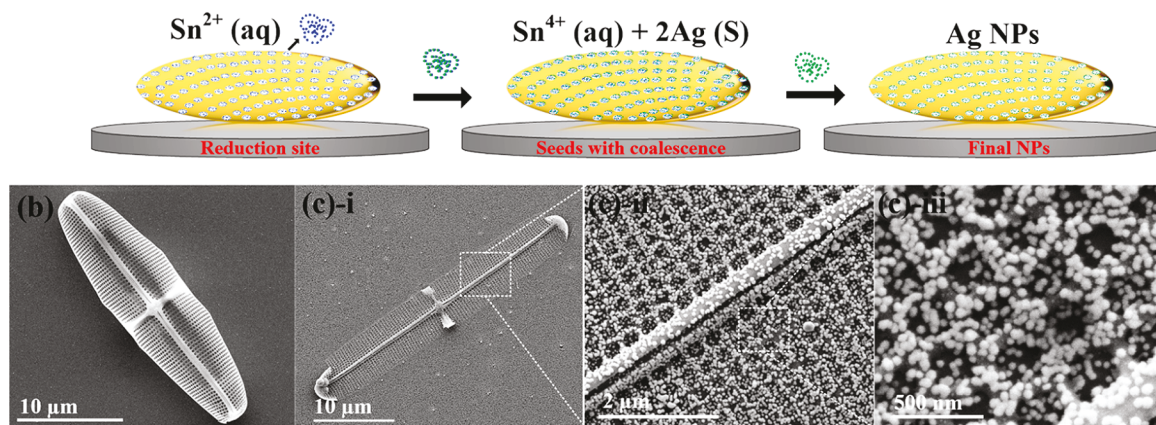


Figure 1. Schematic illustration of Ag NP growth on diatom surface (a). FE-SEM top-view images of diatom (b) and in situ synthesized Ag NPs on diatom surface (c): i-iii various magnifications of the NP-populated diatom.

Many illicit or recreational drugs can be detected using advanced chemistry analysis techniques such as high-performance liquid chromatography, gas chromatography in tandem with mass spectroscopy, and capillary electrophoresis.^{6,8–10,17} Although these methods have excellent sensitivity, they require a sophisticated protocol for sample preparation and suffer long data processing times. Together with high cost, these sensing techniques are inappropriate for quick detection of THC in complex solutions. A simple, rapid, cost-effective, and ultra-sensitive method for the detection of THC in complex biofluids, including blood, urine, and saliva, will therefore play a significant role in various forensic investigations. Surface-enhanced Raman scattering (SERS) is a promising tool for the trace detection of target species at the single-molecule level.^{18–23} With extreme sensitivity and selectivity, it detects these species via inelastic light scattering from the target sample.^{18,19,24,25} Only a few reports have been published on the detection of THC using SERS from regular plasmonic NPs;^{26–29} however, the available SERS reports on THC sensing have been limited to methanol solution for SERS investigations with concentration down to 1 nM. No examination has been undertaken related to the SERS sensing of THC in body fluids (i.e., saliva or plasma) though the detection of THC in body fluids is a primary concern in most drug abuse tests. In particular, THC degrades rapidly in aqueous environments but can be observed in the form of THC metabolite in body fluids. Furthermore, SERS examination of THC metabolite in body fluids would be of significant value for expedited field drug tests. However, the detection of THC or THC metabolite in complex solutions is a challenge when using the SERS platform. Specifically, complex solutions contain multiple biomolecules, which may interfere considerably with the THC SERS signals in lower-concentration detections. Consequently, chemometrics methods, such as principal component analysis (PCA) and the linear regression models, have been applied to classify complex spectral data, which is useful in the accurate identification of THC in body fluids. Additionally, the formation of high-density SERS hotspots remains in demand for detection of THC in complex solutions.

In our previous work, we demonstrated the SERS sensing of various molecules via silver nanoparticles (Ag NPs) coupled

with diatom biosilica surfaces.^{30–32} Metallic NPs deposited near or inside diatom pores form hybrid photonic-plasmonic modes, which can generate a strong local electromagnetic field and enhance SERS signals.^{32–34} In our current study, we present an ultrasensitive hybrid plasmonic-biosilica SERS substrate using high density in situ growth Ag NPs on diatom frustule surface for THC detection in a complex solution. Using this substrate, we achieve THC detection at extremely low concentrations, down to 1 pM, which is 1000 \times lower than the previously best reported results.^{26–29} THC metabolite changes in the body fluid were also analyzed by monitoring the time-dependent SERS spectra. The PCA method was applied to differentiate SERS spectra of THC (1 pM) in methanol, plasma, and purified saliva samples, which proved that the PCA method is necessary to suppress the interference from biofluid background signals. Furthermore, THC (10^{-5} M) in raw saliva solution under various metabolic times was also studied using the PCA method and the linear regression model to estimate the metabolic rate of THC in raw saliva.

EXPERIMENTAL SECTION

Preparation of SERS-Active Substrate. Diatoms were prepared according to a previously published method.^{31,32} The as-prepared diatom substrates were then used for the growth of NPs. In situ synthesized Ag NPs in diatom photonic biosilica were prepared according to our previously published method.³¹ The optimized Ag NP growth concentration, as reported in our previous work, was used to increase the density of NPs in the diatom pores. To increase the density of Ag NPs on diatoms, the NP growth time was increased to 30 min. In brief, the diatom biosilica was first immersed in a solution containing tin(II) chloride (SnCl_2) (20 mM) and hydrochloric acid (HCl) (20 mM) for 30 min to deposit nucleation sites of Sn^{2+} on the diatom surface, before being washed with water and acetone and dried with nitrogen. It was then immersed in a 20 mM aqueous solution of silver nitrate (AgNO_3) for 30 min to grow Ag seeds on the diatom surface. The Ag seeds deposited on the diatom surface were immersed in 1.5 mL of the final growth medium (1 mL of 5 mM AgNO_3 and 0.5 mL of 50 mM ascorbic acid) for 30 min. Impurities were then removed using water and acetone and the substrate was dried with nitrogen. The morphology of Ag NPs on the diatom surface was characterized using field-emission scanning electron microscopy (FE-SEM).

Tetrahydrocannabinol SERS Measurements. The substrates were soaked in 1 mL of various dilutions of the target probe, Rhodamine 6G (R6G) or THC, for 10 min before being dried in air.

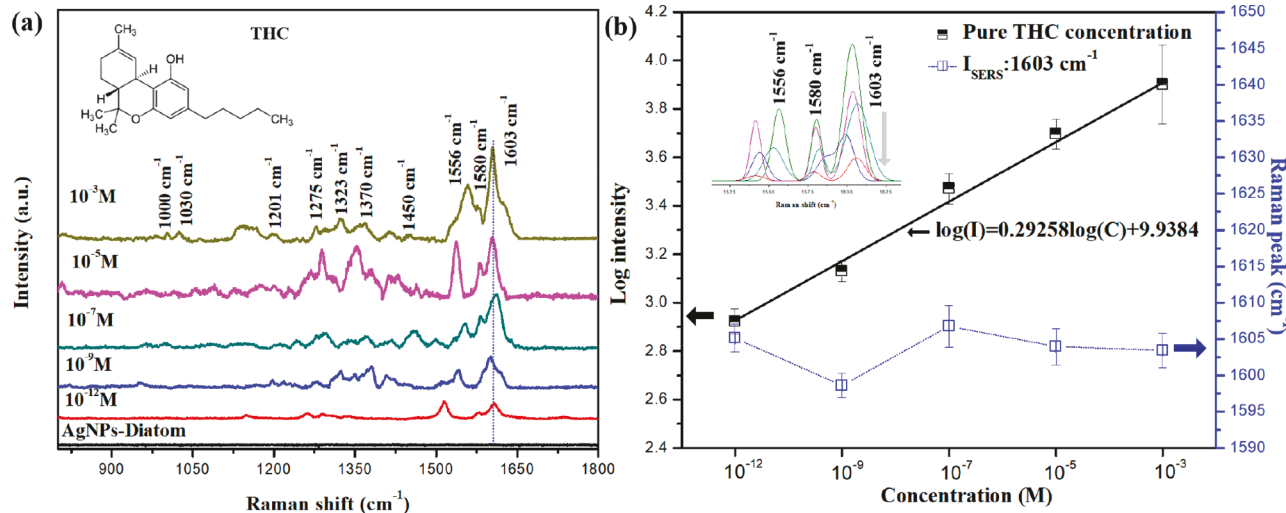


Figure 2. SERS spectra of THC molecules (10^{-3} , 10^{-5} , 10^{-7} , 10^{-9} , and 10^{-12} M) on the plasmonic-biosilica SERS substrate and the inset shows THC molecules chemical structures (a). Left axis: Relationship of I_{SERS} ($\log I$) versus concentration of THC molecules ($\log C$), using I_{SERS} at 1603 cm^{-1} . Right axis: Raman peak shift of I_{SERS} at 1603 cm^{-1} versus concentration of THC; highlighted inset spectra shows the three SERS bands at 1500 – 1700 cm^{-1} (b).

Human plasma solution was obtained from Sigma-Aldrich. THC at various concentrations was mixed with the plasma solution and subjected to SERS detection. Saliva sample were collected from healthy volunteers using an oral swab. The swab wiped the inner mouth for 2 min, collecting ~ 1 mL of saliva, which is denoted as “raw saliva”. The gathered raw saliva (~ 1 mL) was mixed with an equal volume of water and centrifuged for 15 min to remove any food particles from the saliva sample. 500 μL of the centrifuged sample, which was denoted as “purified saliva”, was used for SERS measurements. Various concentrations of THC were added to the raw and purified saliva for quantitative SERS sensing and a study of the metabolic process. Saliva or plasma solutions containing THC were loaded directly onto our hybrid plasmonic-biosilica SERS substrate for measurement, which was conducted using a Raman microscope (Horiba Jobin Yvon Lab Ram HR800). All samples were excited using a 532 nm laser through a 50 \times objective lens with a laser spot size of 2 μm in diameter. Raman spectra were acquired with an integration time of 10 s in the Raman spectral range of 400 to 1800 cm^{-1} .

Multivariate Analysis. Multivariate statistical methods such as the PCA method and partial least-squares regression (PLSR) were used to extract the key features and to explore the spectral variations for the analysis of SERS spectra.^{35–42} In this manuscript, all spectral analysis was performed using MATLAB software. First, all Raman spectra were smoothed using the Z-score method and the background was removed via baseline correction. Three sets of Raman spectra (i.e., pure THC, plasma THC, and purified saliva THC, each with 25 data set) were used for PCA to identify the maximum variation between each data set. The first three PCs (i.e., PC1, PC2, and PC3) were selected as the primary parameters. Similarly, time-dependent THC in raw saliva spectra were analyzed using the first three PCs. PLSR was then applied to predict the outcome at different situations of time-dependent THC concentration in raw saliva.

RESULTS AND DISCUSSION

Characterization of Hybrid Plasmonic-Biosilica Substrate. Figure 1(a) shows the experimental procedure of the in situ growth of Ag NPs on a diatom surface. The diatom biosilica consists of two-dimensional pores with an average diameter of 200 nm, as shown in Figure 1(b). When the diatom biosilica was immersed in aqueous solution containing a SnCl_2 and HCl mixture, nucleation sites of Sn^{2+} ions were deposited on the pore surface of the diatom biosilica surface.

For Ag seed deposition, the Sn^{2+} -deposited diatom surface was immersed in AgNO_3 solution. The reduction of Ag on the diatom surface was achieved using a reduction reaction between Sn^{2+} and two Ag^+ ions, which produced large Ag seeds on the diatom surface and pore walls, as illustrated in Figure 1(a). The uniform-sized Ag NPs were formed from Ag seeds deposited on the diatom surface with the final growth medium (i.e., a mixture of AgNO_3 and ascorbic acid). The Ag NP-populated diatom is shown in Figure 1(c), with i-iii representing various magnifications. The Ag NPs on the diatom surface were spherical in shape and the particle size distribution was obtained from the FE-SEM image. The Ag NPs have average diameters of 40 ± 5 nm as detailed in the Supporting Information (SI). With a growth time of 30 min, high density Ag NPs were formed inside the pores on the diatom surface, generating strong local fields to enhance SERS signals. Strong extinction peaks at 422 and 556 nm are observed, which are correlated to the localized surface plasmonic resonances of Ag NPs-on-diatoms and guided-mode-resonances of the photonic crystal-like diatom frustule respectively, as shown in the SI. SERS spectra of 10^{-6} M R6G from Ag NPs-on-diatom obtained by 532 and 785 nm laser are shown in the SI and it was found that the 532 nm source produced better SERS spectra. The superiority of the SERS spectra from 532 nm laser can be partially attributed to the good spectral overlap between the interrogation wavelength and the photonic structural resonances, allowing for greater optical field enhancement. SERS spectra of various concentrations of R6G on hybrid-plasmonic biosilica SERS substrate obtained by the 532 nm Raman laser are shown in the SI. The strongest characteristic SERS peak of R6G appeared at 1362 cm^{-1} , which was attributed to the C=C stretching modes.⁴³ The Ag NPs on the diatom frustule exhibited ultrahigh SERS effect, which is related to the high density SERS hotspots between Ag NPs. The strong local field presumably occurred at the Ag NPs-inside diatom pores due to the spatially overlapped photonic crystal-plasmonic resonances.^{32,33,44,45}

THC SERS Detection in Methanol Using the Hybrid Plasmonic–Biosilica Substrate. The chemical structure of THC is shown in the inset of Figure 2(a). A stock solution of

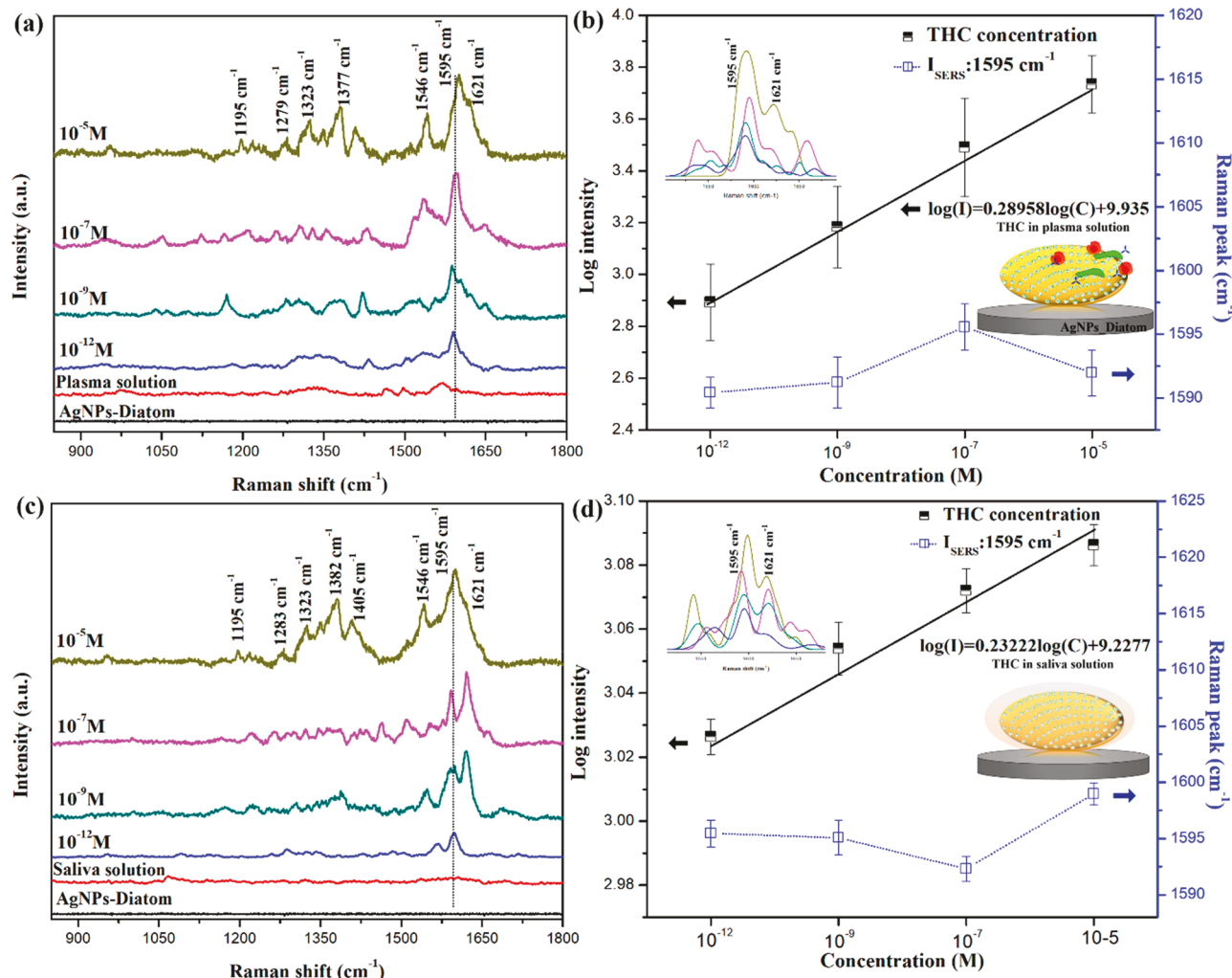


Figure 3. SERS spectra of THC molecules (10^{-5} , 10^{-7} , 10^{-9} , and 10^{-12} M) in plasma (a) and purified saliva solution (c) on the plasmonic-biosilica SERS substrate. I_{SERS} intensities ($\log I$) versus concentration of THC molecules ($\log C$) in plasma (b) and purified saliva solution (d), using I_{SERS} at 1595 cm^{-1} . The right axis of (b) and (d) shows the Raman peak shift of THC at 1595 cm^{-1} versus concentration of THC; highlighted inset spectra shows the SERS bands at $1500\text{--}1700 \text{ cm}^{-1}$ (b,d).

THC (1 mg/mL) in methanol was used to prepare various concentrations of THC, using serial dilution. Hybrid-plasmonic biosilica SERS substrates were soaked in 1 mL of the dilutions of THC in methanol solution for 10 min before being air-dried. The THC solution with concentrations of 10^{-3} to 10^{-12} M on the hybrid plasmonic-biosilica substrates were measured and the results are shown in Figure 2(a). The SERS results show that SERS peaks appeared at 1000, 1030, 1201, 1275, 1323, 1370, 1450, 1556, 1580, and 1603 cm^{-1} as listed in Table S1 in the SI.^{27–29,46,47} The strongest characteristic peak of THC solution appeared at 1603 cm^{-1} , which is attributed to the C=C stretching modes.^{27–29,46,47} Moreover, the other two major SERS bands at 1556 and 1580 cm^{-1} can be used to distinguish THC, which are also attributed to the C=C stretching modes. THC activity is based mainly on the formation of two stereoisomers, i.e., (−)-trans-isomer and (+)-trans-isomer, which generate the strong C=C stretching mode under Raman scattering. Our SERS results are similar to the reported THC spectra.²⁸ Slight shifting of the SERS band to lower and higher wavenumbers was observed at each concentration of THC. Furthermore, the three major SERS peaks of THC at 1556, 1580, and 1603 cm^{-1} were shifted with standard deviation of 3.4, 2.7, and 3.4 cm^{-1} , respectively, as

shown in the inset of Figure 2(b). Figure 2(b) and Figure S6 (SI) show the quantitative relationship between the integrated SERS intensity (I) of 1603 and 1580 cm^{-1} versus the concentration (C) of THC in methanol. A linear response between I and C is obtained with squared correlation coefficients (R^2) of 0.915 for 1580 cm^{-1} and 0.966 for 1603 cm^{-1} . THC solutions of various concentrations (10^{-3} to 10^{-7} M) on Ag NPs on a glass substrate was used as a reference, which were shown in Figure S5 (SI). The SERS enhancement by our hybrid plasmonic-biosilica SERS substrate was higher than that of Ag NPs on glass, achieving a detection limit of THC in methanol down to 10^{-12} M. As a comparison, the Ag NPs on a glass substrate had a THC detection limit of only 10^{-7} M. We attribute the ultrahigh SERS sensitivity to the high density hot spots between Ag NPs in diatom pores, which are also coupled with the photonic crystal resonance of diatom frustules to achieve even higher enhancement factors.

Trace Detection of THC in Complex Solutions. Twenty microliters of plasma solution was added to $20 \mu\text{L}$ of THC solution at various concentrations under vigorous stirring at room temperature to obtain a homogeneous solution. Ag NPs on the diatom substrates were soaked in $40 \mu\text{L}$ of various dilutions of the target probe for 15 min before air-drying. In

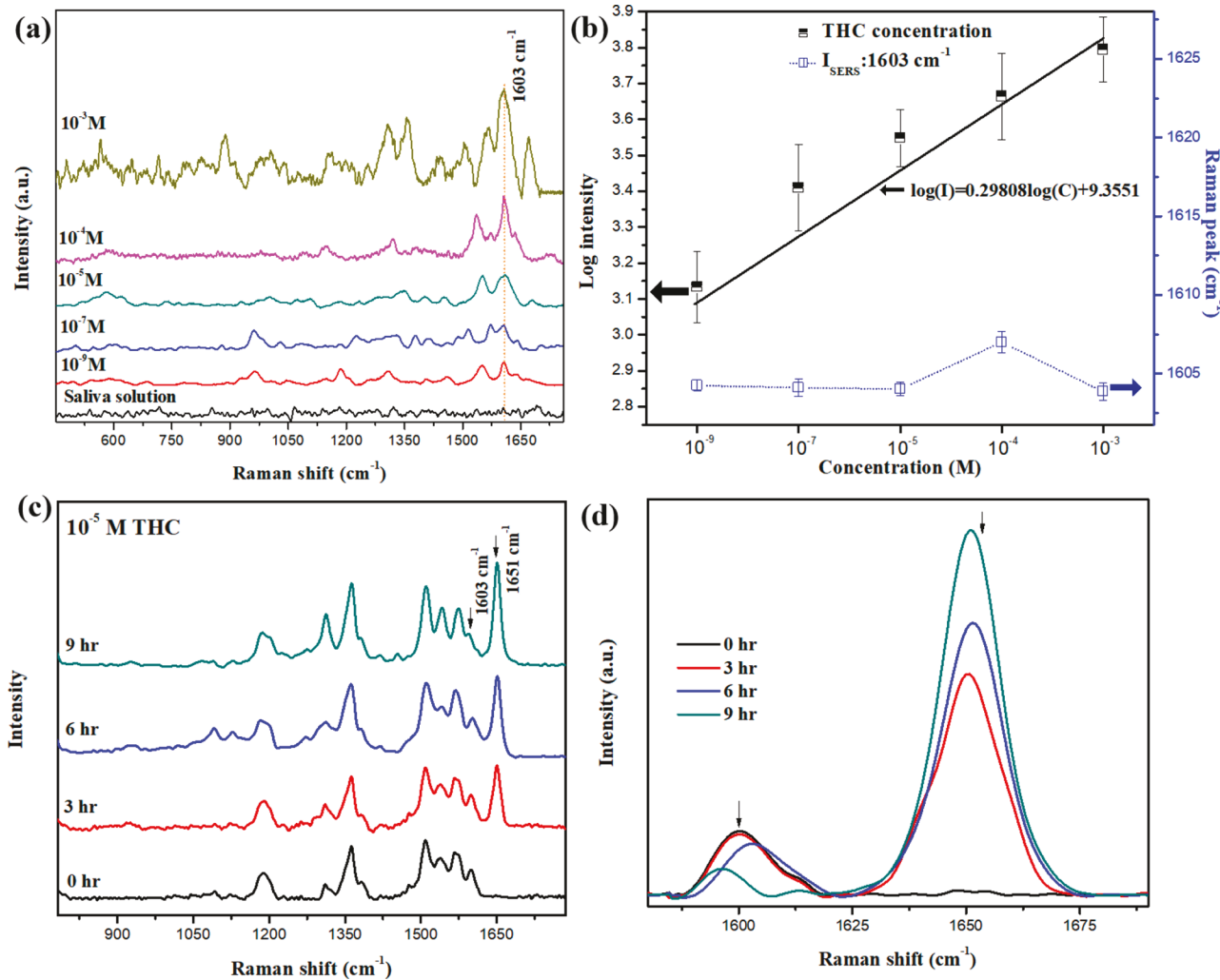


Figure 4. SERS spectra of THC molecules (10^{-3} , 10^{-4} , 10^{-5} , 10^{-7} , and 10^{-9} M) in raw saliva solution on the plasmonic-biosilica SERS substrate (a). I_{SERS} intensities ($\log I$) versus concentration of THC molecules ($\log C$) in raw saliva solution, using I_{SERS} at 1603 cm^{-1} and Raman peak shift of various concentrations of THC versus concentration of THC (b). SERS spectra of 10^{-5} M THC molecules (with various time durations) in raw saliva solution on the plasmonic-biosilica SERS substrate (c) and the Raman spectra at 1550 – 1700 cm^{-1} (d).

Figure 3(a), the SERS spectrum of THC in plasma solution (10^{-3} to 10^{-12} M) exhibits a strong peak at 1595 cm^{-1} , which is assigned to the $\text{C}=\text{C}$ stretching mode.^{27–29,46,47} For the THC in plasma or saliva samples, the SERS spectra significantly changed as a result of rapid oxidization of THC and formation of THC–OH and THC–COOH, which can be used to detect THC in plasma or saliva samples after several hours or even days of intake. The new THC SERS peaks appeared at 1621 cm^{-1} , which were attributed to $\text{O}=\text{C}=\text{O}$ and indicated the formation of a carboxylic acid metabolite (THC–COOH).^{28,48} Thus, the strong $\text{C}=\text{C}$ stretching modes and $\text{O}=\text{C}=\text{O}$ at 1595 and 1621 cm^{-1} can be used to distinguish lower concentrations of THC in plasma solution. The interference from the plasma background signals reduced the THC SERS intensity and a small SERS shift was obtained at 1595 and 1621 cm^{-1} with standard deviation of 2.2 and 4.8 cm^{-1} , respectively, as highlighted in the inset of Figure 3(b). The strong characteristic peaks of THC at 1595 and 1621 cm^{-1} reveal a linear log-scale correlation to the concentration between 10^{-3} M and 10^{-12} M. THC concentration was quantified using the linear eq 1

$$\log(I) = a \log(c) + b \quad (1)$$

where I and C represent the SERS intensity and THC concentration, and a and b are fitting coefficients. R^2 values of 0.998 for 1595 cm^{-1} for 0.99775 and 0.961 for 1621 cm^{-1} were achieved, as shown in Figure 3(b) and Figure S6 (SI). THC in purified saliva solution was also measured by SERS using the hybrid plasmonic-biosilica SERS substrate. Relatively strong SERS bands at 1595 and 1621 cm^{-1} were obtained, as shown in Figure 3(c), and can be attributed to the $\text{C}=\text{C}$ stretching mode and $\text{O}=\text{C}=\text{O}$.^{27–29,46,47} The Ag NPs on the diatom substrate exhibited strong SERS intensities even down to 1 pM concentration. The concentration of THC in the purified saliva sample was quantified using the linear equation with R^2 of 0.971 for 1595 cm^{-1} and 0.983 for 1621 cm^{-1} as shown in Figure 3(d) and Figure S6 (SI). The linear relationship can be used to determine an unknown concentration of THC in plasma or saliva. A small SERS shift was observed at 1595 and 1621 cm^{-1} with standard deviation of 2.7 and 1 cm^{-1} , respectively, as highlighted in the inset of Figure 3(d) due to saliva sample's background signals. In the present work, the detection limit for THC (10^{-12} M) is much better than previously reported values (listed in Table S2).^{27–29,46,47} Thus,

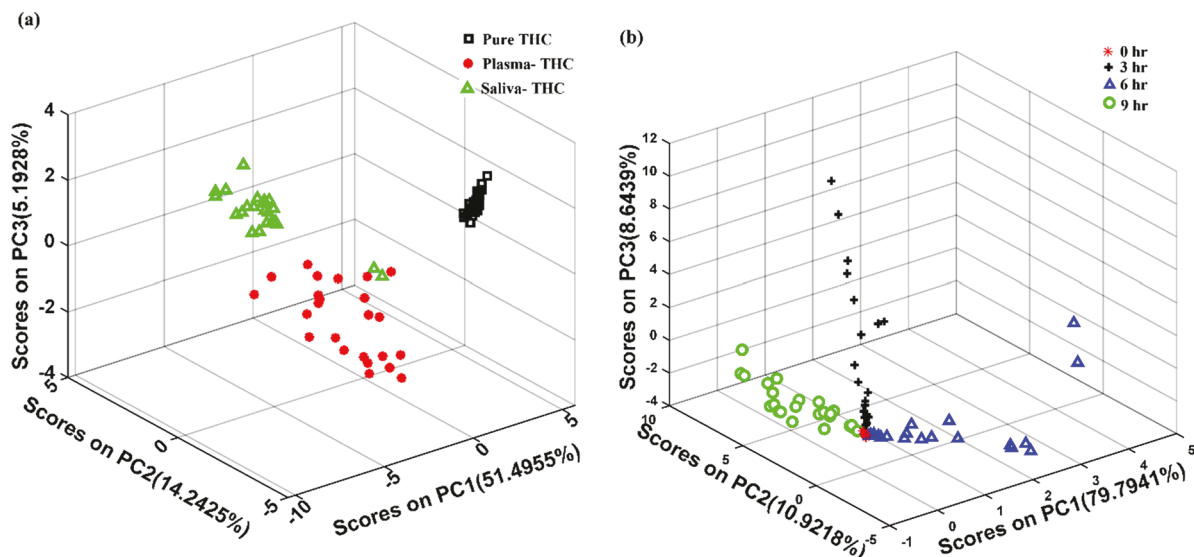


Figure 5. PCA scatter plots of first three PCs for THC (10^{-12} M) in methanol plasma, and purified saliva solution (a) and the metabolic time-dependent THC (10^{-5} M in raw saliva solution) spectra set (b).

our hybrid plasmonic-biosilica SERS substrate is an effective platform for the detection of THC in a complex solution.

Hybrid Plasmonic-Biosilica Substrate for Trace Detection of THC in Raw Saliva Solution. SERS spectra of THC in raw saliva solution (denoted as saliva solution-0 (S0)) with various concentrations (10^{-3} to 10^{-9} M) were also measured using the same setup as earlier. The strong SERS characteristic peaks of THC in raw saliva appeared at 1603 and 1651 cm^{-1} , as shown in Figure 4(a), which are attributed to the C=C stretching mode and O=C=O, respectively.^{27–29,46,47} The O=C=O band obtained at 1651 cm^{-1} could be linked to the THC-COOH because of the strong interaction between proteins or amino groups in raw saliva solution.^{27–29,46,47} The raw saliva THC SERS characteristic peaks shifted slightly between each concentration of THC, which is associated with the raw saliva Raman signal interference, as shown in Figure 4(b). The concentration of THC in raw saliva solution was quantified using the linear equation with R^2 of 0.9558 for 1603 cm^{-1} , as shown in Figure 4(b), which can be used to determine the unknown concentration of THC in raw saliva. These results showed that the lower concentration of THC (1 nM) in raw saliva was distinguished satisfactorily using the hybrid plasmonic-biosilica SERS substrate.

To evaluate the effect of variations among individual saliva samples, we studied THC in saliva from three additional volunteers (denoted as saliva sample-1 (SS1), saliva sample-2 (SS2), and saliva sample-3 (SS3)). Saliva samples were collected from healthy volunteers at different times of the day using an oral swab. THC at various concentrations was added to the raw saliva solutions. The results are shown in Figure S7(a–c). A linear regression was performed to correlate the SERS peak intensity at 1603 cm^{-1} and the THC concentration. R^2 values were achieved of 0.853, 0.849, and 0.881 for SS1, SS2, and SS3, respectively, and is shown in Figure S7(d–f). Furthermore, the Raman peak shift is shown for each saliva sample at various concentrations. Using the THC concentration of 10^{-5} M, we compared the three new saliva samples (SS1–3) with the saliva sample (SS0) used originally. There is a certain level of variation among the SERS

spectra from each saliva sample in the 900 – 1500 cm^{-1} region, which is due to the difference of the saliva sample, as would be expected. However, the characteristic peak at 1603 cm^{-1} is distinguishable and remains relatively constant. The intensity and Raman shift of the characteristic peaks from the C=C stretching for the four saliva samples were compared and a relatively large intensity variation occurred between SS0 and SS1–3. This is most likely caused by the difference of the SERS substrates. The difference of the Raman peak wavenumber among all samples, however, is very minimal and even smaller than the standard deviation of each sample. This proves that the variation of THC signals in the same type of biofluidic sample from different people is acceptable.

We also investigated the THC metabolite changes at various time periods (i.e., 0, 3, 6, and 9 h) with a concentration of 10^{-5} M THC in raw saliva solution. SERS characteristic peaks of THC were greatly influenced by the time-dependent SERS measurement, as shown in Figure 4(c,d). Notable THC metabolite changes are highly present in real body fluids (raw saliva) after several hours of THC intake. Figure 4(c,d) shows the progression of time of THC in raw saliva from 0 to 9 h, and the formation of the strong O=C=O band at 1651 cm^{-1} due to significant changes in the THC structure. Moreover, the THC SERS characteristic peak intensity of 1603 cm^{-1} was notably reduced while increasing the THC time in raw saliva. Thus, the THC metabolite changes could be a better indicator to detect THC in body fluids using SERS sensing.

PCA and PLSR Analysis. Two independent PCA processes were applied for different types of analysis. The first PCA process was conducted by extracting the principal components of the SERS spectra among different solvents to account for the effect of solvents. The date set include SERS spectra of the three samples at 10^{-12} M concentration of THC in methanol, plasma, and purified saliva. The SERS spectral region of interest is between 400 and 1800 cm^{-1} for all samples to identify the maximum variations of each data set. The first three principal components (PCs) at 51.49% (PC1), 14.24% (PC2), and 5% (PC3) of the variance were obtained and plotted in Figure 5(a). The three separate clusters clearly show

the separation of THC in various solutions, reflecting the impact of different biological background signals.

The second PCA process was conducted by extracting the principal components among SERS spectra of THC in saliva at different times to account for the metabolic decomposition and oxidation of THC. The metabolic times of 0, 3, 6, and 9 h of 10^{-5} M THC in raw saliva samples were analyzed. The first three PCs of the SERS spectra account for 98% of the variance for different THC metabolic time, which are 79.79% (PC1), 10.92% (PC2), and 8.64% (PC3) as shown in Figure 5(b). At the metabolic time of 0 h, the spectra in the PC space are densely packed, forming a tight cluster. As the structure of THC changes into hydroxyl or carboxylic acids due to the metabolic process, the resulting SERS spectra spread into narrow clusters along distinct directions. These discrete narrow clusters, seen in Figure 5(b), allow for clear identification of individual characteristics of time-dependent THC metabolic changes in raw saliva samples. This can be useful for semiquantitative classification to determine the extent of THC metabolic process. Similarly, the time-dependent nature of SERS spectra for 10^{-5} M THC in phosphate buffered saline (PBS) solution was investigated and the results are shown in Figure S9(a,b) in the SI. This analysis shows the time dependence of THC hydroxylation in PBS solution, which is different from the metabolic process in raw saliva. At the beginning, THC in PBS solution generated the typical SERS signature peak at 1595 cm^{-1} . However, as time progresses, the THC molecule is altered due to hydrolysis in the PBS solution. The hydrolysis process produces a new SERS peak at 1616 cm^{-1} , which is different than the SERS peak at 1651 cm^{-1} due to hydroxylation and metabolism in raw saliva. More detailed discussion can be found in the SI.

The linear regression model was used to estimate the decay time of THC in raw saliva, as shown in Figure 6 below. PLSR can provide accurate predication, using the root mean squared error (RMSE) as our metric. A 5-fold cross-validation was employed where 80% of the time decay data was used for calibration while 20% was used to test the predictive

capabilities of the model. The calibration and test data set achieved RMSE values of 0.9318 and 1.2833 and R^2 values of 0.9820 and 0.8305, respectively, indicating a good linear fit for the model. The predicted decay times in the testing data set were well matched. Thus, the time-dependent results by the PCA and PLSR methods can be used to characterize the THC metabolic behavior in raw saliva after several hours of intake of THC.

CONCLUSION

In this paper, we reported the trace detection of THC, which is the main active component in marijuana, from complex body fluids using SERS-active substrates based on hybrid plasmonic-biosilica nanomaterials. We achieved ultralow detection of THC down to 1 pM in plasma and purified saliva solutions, which is at least 3 orders of magnitude better than the best results in methanol reported by other groups. The strong SERS characteristic peak of THC in methanol solution was obtained at 1603 cm^{-1} with standard deviation of 3.4 cm^{-1} and this signature peak shows a noticeable wavenumber shift in the plasma and saliva solution. Additionally, THC in plasma or purified saliva samples produces a strong SERS peak at 1621 cm^{-1} due to the stretching mode of $\text{O}-\text{C}=\text{O}$, which results from the metabolic change of THC structures in body fluids after several hours of THC intake. The maximum variability of the first three principal components was achieved at 71% for THC in methanol, plasma, and purified saliva solution for the identification in complex solutions. THC in raw saliva solution under various metabolic times was also studied by PCA and 98% of maximum variations were obtained, yielding time-dependent information on the THC metabolic changes in body fluids. A linear regression model was then used to successfully estimate the metabolic rate of THC in raw saliva. Thus, the hybrid plasmonic-biosilica SERS substrate has the potential to monitor THC or THC metabolic changes in body fluids after different times of drug use.

ASSOCIATED CONTENT

Supporting Information

The Supporting Information is available free of charge on the ACS Publications website at DOI: [10.1021/acssensors.9b00476](https://doi.org/10.1021/acssensors.9b00476).

Further description of the SERS characterization of plasmonic-biosilica substrate and SERS characterization of THC in complex solution ([PDF](#))

AUTHOR INFORMATION

Corresponding Author

*E-mail: wang@oregonstate.edu.

ORCID

Alan X. Wang: [0000-0002-0553-498X](https://orcid.org/0000-0002-0553-498X)

Notes

The authors declare no competing financial interest.

ACKNOWLEDGMENTS

This work was financially supported by the National Institutes of Health under Grant No. 1R21DA0437131, the National Science Foundation under Grant No. 1701329, and the United States Department of Agriculture under Grant No. 2017-67021-26606.

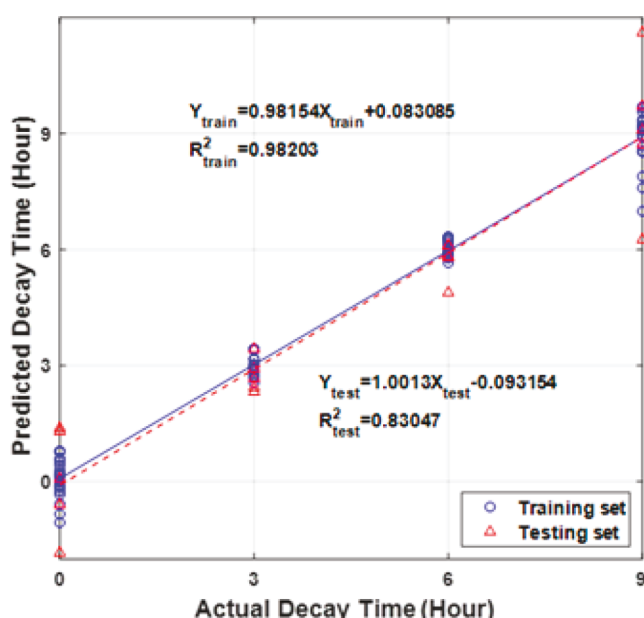


Figure 6. Correlation between the actual and predicted time decay of THC in raw saliva samples for training and test data sets.

■ REFERENCES

(1) Koppel, B. S.; Brust, J. C. M.; Fife, T.; Bronstein, J.; Youssof, S.; Gronseth, G.; Gloss, D. Systematic review: Efficacy and safety of medical marijuana in selected neurologic disorders. *Neurology* **2014**, *82* (17), 1556–1563.

(2) Lee, J.-R.; Choi, J.; Shultz, T. O.; Wang, S. X. Small Molecule Detection in Saliva Facilitates Portable Tests of Marijuana Abuse. *Anal. Chem.* **2016**, *88* (15), 7457–7461.

(3) Murray, R. M.; Morrison, P. D.; Henquet, C.; Forti, M. D. Cannabis, the mind and society: the hash realities. *Nat. Rev. Neurosci.* **2007**, *8*, 885.

(4) Zuardi, A. W. History of cannabis as a medicine: a review. *Revista Brasileira de Psiquiatria* **2006**, *28*, 153–157.

(5) Kalant, H. Medicinal Use of Cannabis: History and Current Status. *Pain Research and Management* **2001**, *6* (2), 80–91.

(6) Kim, S. Y.; Kim, J. Y.; Kwon, W.; In, M. K.; Kim, Y. E.; Paeng, K.-J. Method development for simultaneous determination of amphetamine type stimulants and cannabinoids in urine using GC–MS. *Microchem. J.* **2013**, *110*, 326–333.

(7) Wei, B.; Wang, L.; Blount, B. C. Analysis of Cannabinoids and Their Metabolites in Human Urine. *Anal. Chem.* **2015**, *87* (20), 10183–10187.

(8) Grauwiler, S. B.; Scholer, A.; Drewe, J. Development of a LC/MS/MS method for the analysis of cannabinoids in human EDTA-plasma and urine after small doses of *Cannabis sativa* extracts. *J. Chromatogr. B: Anal. Technol. Biomed. Life Sci.* **2007**, *850* (1), 515–522.

(9) Lurie, I. S.; Meyers, R. P.; Conver, T. S. Capillary Electrophoresis of Cannabinoids. *Anal. Chem.* **1998**, *70* (15), 3255–3260.

(10) Ambach, L.; Penitschka, F.; Broillet, A.; König, S.; Weinmann, W.; Bernhard, W. Simultaneous quantification of delta-9-THC, THC-acid A, CBN and CBD in seized drugs using HPLC-DAD. *Forensic Sci. Int.* **2014**, *243*, 107–111.

(11) Tose, L. V.; Santos, N. A.; Rodrigues, R. R. T.; Murgu, M.; Gomes, A. F.; Vasconcelos, G. A.; Souza, P. C. T.; Vaz, B. G.; Romão, W. Isomeric separation of cannabinoids by UPLC combined with ionic mobility mass spectrometry (TWIM-MS)—Part I. *Int. J. Mass Spectrom.* **2017**, *418*, 112–121.

(12) Zgair, A.; Wong, J. C. M.; Sabri, A.; Fischer, P. M.; Barrett, D. A.; Constantinescu, C. S.; Gershkovich, P. Development of a simple and sensitive HPLC–UV method for the simultaneous determination of cannabidiol and $\Delta 9$ -tetrahydrocannabinol in rat plasma. *J. Pharm. Biomed. Anal.* **2015**, *114*, 145–151.

(13) Wohlfarth, A.; Mahler, H.; Auwärter, V. Rapid isolation procedure for $\Delta 9$ -tetrahydrocannabinolic acid A (THCA) from *Cannabis sativa* using two flash chromatography systems. *J. Chromatogr. B: Anal. Technol. Biomed. Life Sci.* **2011**, *879* (28), 3059–3064.

(14) Colizzi, M.; Bhattacharyya, S. Does Cannabis Composition Matter? Differential Effects of Delta-9-tetrahydrocannabinol and Cannabidiol on Human Cognition. *Current Addiction Reports* **2017**, *4* (2), 62–74.

(15) Bloomfield, M. A. P.; Ashok, A. H.; Volkow, N. D.; Howes, O. D. The effects of $\Delta 9$ -tetrahydrocannabinol on the dopamine system. *Nature* **2016**, *539*, 369.

(16) Sultan, S.; Millar, S.; O'Sullivan, S.; England, T. A Systematic Review and Meta-Analysis of the In Vivo Haemodynamic Effects of $\Delta 9$ -Tetrahydrocannabinol. *Pharmaceuticals* **2018**, *11* (1), 13.

(17) Groeneveld, G.; de Puit, M.; Bleay, S.; Bradshaw, R.; Francese, S. Detection and mapping of illicit drugs and their metabolites in fingermarks by MALDI MS and compatibility with forensic techniques. *Sci. Rep.* **2015**, *5*, 11716.

(18) Li, W.; Zhao, X.; Yi, Z.; Glushenkov, A. M.; Kong, L. Plasmonic substrates for surface enhanced Raman scattering. *Anal. Chim. Acta* **2017**, *984*, 19–41.

(19) Luo, S.-C.; Sivashanmugan, K.; Liao, J.-D.; Yao, C.-K.; Peng, H.-C. Nanofabricated SERS-active substrates for single-molecule to virus detection in vitro: A review. *Biosens. Bioelectron.* **2014**, *61*, 232–240.

(20) Liu, H.-L.; Cao, J.; Hanif, S.; Yuan, C.; Pang, J.; Levicky, R.; Xia, X.-H.; Wang, K. Size-Controllable Gold Nanopores with High SERS Activity. *Anal. Chem.* **2017**, *89* (19), 10407–10413.

(21) Peksa, V.; Jahn, M.; Štolcová, L.; Schulz, V.; Proška, J.; Procházka, M.; Weber, K.; Cialla-May, D.; Popp, J. Quantitative SERS Analysis of Azorubine (E 122) in Sweet Drinks. *Anal. Chem.* **2015**, *87* (5), 2840–2844.

(22) Scott, B. L.; Carron, K. T. Dynamic Surface Enhanced Raman Spectroscopy (SERS): Extracting SERS from Normal Raman Scattering. *Anal. Chem.* **2012**, *84* (20), 8448–8451.

(23) Wang, Z.; Zong, S.; Wu, L.; Zhu, D.; Cui, Y. SERS-Activated Platforms for Immunoassay: Probes, Encoding Methods, and Applications. *Chem. Rev.* **2017**, *117* (12), 7910–7963.

(24) Xu, X.; Li, H.; Hasan, D.; Ruoff, R. S.; Wang, A. X.; Fan, D. L. Near-Field Enhanced Plasmonic-Magnetic Bifunctional Nanotubes for Single Cell Bioanalysis. *Adv. Funct. Mater.* **2013**, *23* (35), 4332–4338.

(25) Zhang, N.; Liu, K.; Liu, Z.; Song, H.; Zeng, X.; Ji, D.; Cheney, A.; Jiang, S.; Gan, Q. Ultrabroadband Metasurface for Efficient Light Trapping and Localization: A Universal Surface-Enhanced Raman Spectroscopy Substrate for “All” Excitation Wavelengths. *Adv. Mater. Interfaces* **2015**, *2* (10), 1500142.

(26) Doctor, E. L.; McCord, B. The application of supported liquid extraction in the analysis of benzodiazepines using surface enhanced Raman spectroscopy. *Talanta* **2015**, *144*, 938–943.

(27) Islam, S. K.; Cheng, Y. P.; Birke, R. L.; Green, O.; Kubic, T.; Lombardi, J. R. Rapid and sensitive detection of synthetic cannabinoids AMB-FUBINACA and α -PVP using surface enhanced Raman scattering (SERS). *Chem. Phys.* **2018**, *506*, 31–35.

(28) Yüksel, S.; Schwenke, A. M.; Soliveri, G.; Ardiizzone, S.; Weber, K.; Cialla-May, D.; Hoeppener, S.; Schubert, U. S.; Popp, J. Trace detection of tetrahydrocannabinol (THC) with a SERS-based capillary platform prepared by the in situ microwave synthesis of AgNPs. *Anal. Chim. Acta* **2016**, *939*, 93–100.

(29) Milliken, S.; Fraser, J.; Poirier, S.; Hulse, J.; Tay, L.-L. Self-assembled vertically aligned Au nanorod arrays for surface-enhanced Raman scattering (SERS) detection of Cannabinol. *Spectrochim. Acta, Part A* **2018**, *196*, 222–228.

(30) Kong, X.; Chong, X.; Squire, K.; Wang, A. X. Microfluidic diatomite analytical devices for illicit drug sensing with ppb-level sensitivity. *Sens. Actuators, B* **2018**, *259*, 587–595.

(31) Kong, X.; Xi, Y.; Le Duff, P.; Chong, X.; Li, E.; Ren, F.; Rorrer, G. L.; Wang, A. X. Detecting explosive molecules from nanoliter solution: A new paradigm of SERS sensing on hydrophilic photonic crystal biosilica. *Biosens. Bioelectron.* **2017**, *88*, 63–70.

(32) Kong, X.; Xi, Y.; LeDuff, P.; Li, E.; Liu, Y.; Cheng, L.-J.; Rorrer, G. L.; Tan, H.; Wang, A. X. Optofluidic sensing from inkjet-printed droplets: the enormous enhancement by evaporation-induced spontaneous flow on photonic crystal biosilica. *Nanoscale* **2016**, *8* (39), 17285–17294.

(33) Kong, X.; Squire, K.; Li, E.; LeDuff, P.; Rorrer, G. L.; Tang, S.; Chen, B.; McKay, C. P.; Navarro-Gonzalez, R.; Wang, A. X. Chemical and Biological Sensing Using Diatom Photonic Crystal Biosilica With In-Situ Growth Plasmonic Nanoparticles. *IEEE Transactions on NanoBioscience* **2016**, *15* (8), 828–834.

(34) Ren, F.; Campbell, J.; Wang, X.; Rorrer, G. L.; Wang, A. X. Enhancing surface plasmon resonances of metallic nanoparticles by diatom biosilica. *Opt. Express* **2013**, *21* (13), 15308–15313.

(35) Chen, J.; Liu, M.; Yuan, H.; Huang, S.; Zhao, J.; Tao, J.; Xu, N. Surface-enhanced Raman spectroscopy for classification of testosterone propionate and nandrolone residues in chicken. *Vib. Spectrosc.* **2018**, *99*, 7–12.

(36) Connolly, J. M.; Davies, K.; Kazakeviciute, A.; Wheatley, A. M.; Dockery, P.; Keogh, I.; Olivo, M. Non-invasive and label-free detection of oral squamous cell carcinoma using saliva surface-enhanced Raman spectroscopy and multivariate analysis. *Nanomedicine* **2016**, *12* (6), 1593–1601.

(37) Kamińska, A.; Witkowska, E.; Kowalska, A.; Skoczyńska, A.; Ronkiewicz, P.; Szymborski, T.; Waluk, J. Rapid detection and identification of bacterial meningitis pathogens in ex vivo clinical samples by SERS method and principal component analysis. *Anal. Methods* **2016**, *8* (22), 4521–4529.

(38) Shizhuang, W.; Sheng, C.; Miao, L.; Xinhua, Z.; Shouguo, Z.; Jian, Z.; Jin, C.; Lei, C. Quantitative analysis of thiram based on SERS and PLSR combined with wavenumber selection. *Anal. Methods* **2014**, *6* (1), 242–247.

(39) Chen, X.; Nguyen, T. H. D.; Gu, L.; Lin, M. Use of Standing Gold Nanorods for Detection of Malachite Green and Crystal Violet in Fish by SERS. *J. Food Sci.* **2017**, *82* (7), 1640–1646.

(40) Gracie, K.; Correa, E.; Mabbott, S.; Dougan, J. A.; Graham, D.; Goodacre, R.; Faulds, K. Simultaneous detection and quantification of three bacterial meningitis pathogens by SERS. *Chemical Science* **2014**, *5* (3), 1030–1040.

(41) Kotanen, C. N.; Martinez, L.; Alvarez, R.; Simecek, J. W. Surface enhanced Raman scattering spectroscopy for detection and identification of microbial pathogens isolated from human serum. *Sensing and Bio-Sensing Research* **2016**, *8*, 20–26.

(42) Zou, S.; Hou, M.; Li, J.; Ma, L.; Zhang, Z. Semi-quantitative analysis of multiple chemical mixtures in solution at trace level by surface-enhanced Raman Scattering. *Sci. Rep.* **2017**, *7* (1), 6186.

(43) Sivashanmugan, K.; Liao, J.-D.; You, J.-W.; Wu, C.-L. Focused-ion-beam-fabricated Au/Ag multilayered nanorod array as SERS-active substrate for virus strain detection. *Sens. Actuators, B* **2013**, *181*, 361–367.

(44) Yang, J.; Zhen, L.; Ren, F.; Campbell, J.; Rorrer, G. L.; Wang, A. X. Ultra-sensitive immunoassay biosensors using hybrid plasmonic-biosilica nanostructured materials. *Journal of Biophotonics* **2015**, *8* (8), 659–667.

(45) Qi, J.; Motwani, P.; Gheewala, M.; Brennan, C.; Wolfe, J. C.; Shih, W.-C. Surface-enhanced Raman spectroscopy with monolithic nanoporous gold disk substrates. *Nanoscale* **2013**, *5* (10), 4105–4109.

(46) Mostowt, T.; McCord, B. Surface enhanced Raman spectroscopy (SERS) as a method for the toxicological analysis of synthetic cannabinoids. *Talanta* **2017**, *164*, 396–402.

(47) Dies, H.; Raveendran, J.; Escobedo, C.; Docolis, A. Rapid identification and quantification of illicit drugs on nanodendritic surface-enhanced Raman scattering substrates. *Sens. Actuators, B* **2018**, *257*, 382–388.

(48) Sivashanmugan, K.; Liu, P.-C.; Tsai, K.-W.; Chou, Y.-N.; Lin, C.-H.; Chang, Y.; Wen, T.-C. An anti-fouling nanoplasmonic SERS substrate for trapping and releasing a cationic fluorescent tag from human blood solution. *Nanoscale* **2017**, *9* (8), 2865–2874.